Neuro-Oncology 13(8):866–879, 2011.
doi:10.1093/neuonc/nor070

Genome-wide molecular characterization of central nervous system primitive neuroectodermal tumor and pineoblastoma

Suzanne Miller, Hazel A. Rogers, Paul Lyon, Vikki Rand, Martyna Adamowicz-Brice, Steven C. Clifford, James T. Hayden, Sara Dyer, Stefan Pfister, Andrey Korshunov, Marie-Anne Brundler, James Lowe, Beth Coyle, and Richard G. Grundy

Children's Brain Tumour Research Centre, School of Clinical Sciences, Queen's Medical Centre, University of Nottingham (S.M., H.A.R., P.L., V.R., M.A-B., S.D., J.L., B.C., R.G.G.), and Department of Neuropathology, Nottingham University Hospital, Queens Medical Centre, Nottingham, United Kingdom (J.L.); Northern Institute for Cancer Research, Newcastle University, Newcastle Upon Tyne (V.R., S.C.C., J.T.H.), West Midlands Regional Genetic Laboratory, Birmingham Women's Hospital (S.D.), and Department of Pathology, Birmingham Children's Hospital (M-A.B.), Birmingham, United Kingdom; Division of Molecular Genetics (S.P.) and Clinical Cooperation Unit Neuropathology (A.K.), German Cancer Research Centre, and Paediatric Haematology and Oncology, Heidelberg University Hospital (S.P.), Heidelberg, Germany

Central nervous system primitive neuroectodermal tumor (CNS PNET) and pineoblastoma are highly malignant embryonal brain tumors with poor prognoses. Current therapies are based on the treatment of pediatric medulloblastoma, even though these tumors are distinct at both the anatomical and molecular level. CNS PNET and pineoblastoma have a worse clinical outcome than medulloblastoma; thus, improved therapies based on an understanding of the underlying biology of CNS PNET and pineoblastoma are needed. To this end, we characterized the genomic alterations of 36 pediatric CNS PNETs and 8 pineoblastomas using Affymetrix single nucleotide polymorphism arrays. Overall, the majority of CNS PNETs contained a greater degree of genomic imbalance than pineoblastomas, with gain of 19p (8 [27.6%] of 29), 2p (7 [24.1%] of 29), and 1q (6 [20.7%] of 29) common events in primary CNS PNETs. Novel gene copy number alterations were identified and corroborated by Genomic Identification of Significant Targets In Cancer (GISTIC) analysis: gain of *PCDHGA3*, 5q31.3 in 62.1% of primary CNS PNETs and all primary pineoblastomas and *FAM129A*, 1q25 in 55.2% of primary CNS PNETs and 50% of primary pineoblastomas. Comparison of our GISTIC data with publically available data for medulloblastoma confirmed these CNS PNET–specific copy number alterations. With use of the collection of 5 primary and recurrent CNS PNET pairs, we found that gain of 2p21 was maintained at relapse in 80% of cases. Novel gene copy number losses included *OR4C12*, 11p11.12 in 48.2% of primary CNS PNETs and 50% of primary pineoblastomas. Loss of *CDKN2A/B* (9p21.3) was identified in 14% of primary CNS PNETs and was significantly associated with older age among children ($P = .05$). *CADPS*, 3p14.2 was lost in 27.6% of primary CNS PNETs and was associated with poor prognosis ($P = .043$). This genome-wide analysis revealed the marked molecular heterogeneity of CNS PNETs and enabled the identification of novel genes and clinical associations potentially involved in the pathogenesis of these tumors.

Keywords: *CDKN2A/CDKN2B*, CNS PNET, copy number imbalance, pineoblastoma, SNP array.

The comprehensive molecular characterization of central nervous system primitive neuroectodermal tumors (CNS PNETs) has been hindered by their relative rarity, the challenge of performing small-tumor biopsies from surgically inaccessible anatomical locations, and heterogeneous histological and clinical characteriztics. Of PNETs arising in the supratentorial compartment of the brain, 80% arise in cerebral or suprasellar regions (CNS PNET), whereas 20% are located in the pineal region (pineoblastoma).[1,2] CNS PNET and pineoblastoma have similar histological characteristics, being highly heterogeneous tumors with

Received August 23, 2010; accepted April 7, 2011.

Corresponding Author: Professor Richard Grundy, Children's Brain Tumour Research Centre, Queen's Medical Centre, University of Nottingham, Nottingham, NG7 2UH, United Kingdom (richard.grundy@nottingham.ac.uk).

scant cytoplasm.[3] Anatomical distribution of these supratentorial tumors differs with patient age. Pineoblastomas more commonly arise in children aged <3 years. For children aged ≥3 years, a pineal location is associated with better outcome than CNS PNETs, whereas both pineal region and cortical tumors in children aged <3 years have a very poor prognosis.[1,4,5] Conversely, patients aged ≥3 years with pineal tumors have a survival rate of >70%.[5] Until recently, CNS PNET and pineoblastoma have been treated in a similar, age-dependent manner as their more common infratentorial counterpart, medulloblastoma.[4,5] However, it is now clear that, overall, patients with CNS PNET or with pineoblastoma have a worse prognosis than those diagnosed with medulloblastoma.[4–6]

Emerging data from cytogenetic and molecular genetic analyses suggest that CNS PNETs are genetically distinct from medulloblastoma.[7–10] However, a recent study reported similarities in the tumorigenesis of CNS PNET and medulloblastoma. WNT/beta-catenin pathway activation was observed in both CNS PNET and medulloblastoma, although the mechanisms behind WNT/beta-catenin pathway activation may differ.[11] Cytogenetic analysis has revealed that CNS PNETs have complex karyotypes with many unbalanced rearrangements.[12–20] However, too few CNS PNETs and pineoblastomas have been analyzed to identify specific genomic alterations. In total 16 pediatric cases analyzed by conventional CGH and a further 17 cases analyzed using array CGH have been reported in the literature.[7–9,13,21–23] Compilation of aCGH and fluorescence in situ hybridization (FISH) analyses has shown loss of 9p21.3 (encompassing *CDKN2A* and *CDKN2B*) to be a frequent event in CNS PNET.[9] More recently, genomic profiling of 39 primary CNS PNETs using 500K single nucleotide polymorphism (SNP) arrays revealed that CNS PNETs contained numerous copy number alterations and that the tumors displayed marked genomic heterogeneity.[10] Even so, recurrent gains of chromosome 2 and focal amplification of 19q13.41 were observed in 8 (20.5%) of 39 primary CNS PNETs. Here, we present data on a cohort of 36 CNS PNETs and 8 pineoblastomas using 100K and 500K Affymetrix SNP arrays to identify genome-wide copy number imbalance. Genomic Identification of Significant Targets In Cancer (GISTIC) analysis was used to identify genes of interest and to aid the molecular distinction from medulloblastoma. Importantly, the collection of clinical information, along with the investigation of gene copy number imbalance, allowed comparisons to be made, linking specific imbalances with clinically related patient groups. The inclusion of 5 primary and recurrent CNS PNET pairs enabled the characterization of maintained and acquired copy number alterations.

Materials and Methods

Clinical Samples Entered into the SNP Array Analysis

Forty-four samples (35 snap-frozen CNS PNETs, 8 snap-frozen pineoblastomas, and 1 CNS PNET cell line) were obtained for analysis using the Affymetrix SNP arrays (Affymetrix). Of the 35 CNS PNET samples collected, 29 were primary tumors, whereas 6 were recurrent tumors (5 of which were paired with a primary sample from the same patient). The age of patients with CNS PNET ranged from 10 to 190 months, with mean and median ages of 68.7 and 60 months, respectively, at diagnosis. Included within the CNS PNET cohort was a commercially available CNS PNET cell line, PFSK1 (CRL-2060, ATCC). Of 8 pineoblastomas collected, 6 were primary tumors and 2 were recurrent tumors with no primary tumor available. The age of patients with pineoblastoma ranged from 6 to 168 months, with mean and median ages of 49.25 and 19.5 months, respectively. Fourteen constitutional blood samples (paired with CNS PNET 9, 10, 15, 26, 31, 33, 34, 35, 36, 38, 39, and 43 and PB 3 and 4) were available for normalization purposes. Samples and clinical information were collected from 6 Children's Cancer and Leukaemia Group–registered centers in the United Kingdom, in addition to the Cooperative Human Tissue Network (CHTN) in America. The study met with Multiple Centre Research Committee approval, and consent was provided to obtain tumor samples in accordance with national banking procedures and the human tissue act. Tumors were histopathologically reviewed at each center in accordance with World Health Organization (WHO) criteria of the time.

Tumor Material and DNA Isolation

Ten milligrams of tissue was cut for each sample for DNA extraction, and a tissue smear prepared from the same area of tumor for a central histopathological review by at least 3 pathologists using the most recent WHO criteria.[3] After microscopic evaluation, only tumor samples containing >90% viable tumor had DNA extracted. A standard phenol/chloroform/isoamyl alcohol method was used. Constitutional DNA (used in the normalization of SNP array data) was extracted using the same method after red blood cell lysis in water and centrifugation.

Affymetrix 100K and 500K Mapping Sets and Data Analysis

***Data generation*—**Twenty-four CNS PNETs and 8 pineoblastomas were analyzed using the genechip human mapping 100K set (Affymetrix) to identify genome-wide copy number alterations. On the release of the genechip human mapping 500K set, an additional 11 CNS PNETs and 1 CNS PNET cell line (PFSK1) were analyzed. DNA digestion, labeling, and hybridization were performed on the basis of the Affymetrix 100K or 500K SNP array protocols.[24,25] In brief, 250 ng of DNA was digested (with either Xba1 or HindIII [New England Biolabs] for each 50K SNP array and NspI or StyI [New England Biolabs] for each 250K SNP array). After adaptor ligation, samples were amplified by polymerase chain reaction (PCR) using Titanium *Taq* DNA

polymerase (Clontech) for the 100K assay or AmpliTag Gold (Applied Biosystems) for the 500K assay. Pooled and concentrated amplified PCR products were then fragmented, labeled, denatured, and hybridized for 16 h. Arrays were subsequently washed (Affymetrix Fluidics station 450) and scanned (Affymetrix Genechip Scanner 3000).

Data analysis.—Affymetrix CEL files were generated using Affymetrix Genotyping Analysis Software (GTYPE 4.1). In the generation of CHP files, the dynamic model was used for the 100K analysis, and the Bayesian robust linear model with mahalanobis was used for the 500K analysis. To identify copy number aberrations, CEL and CHP files were imported into Copy Number Analyzer for Affymetrix Genechip (CNAG) version 2.0.[26] For paired samples (14 tumors had matched constitutional DNA) tumor data were normalized using the corresponding paired reference, and the unpaired tumor data were normalized against 270 HAPMAP samples,[27] allowing for the identification of tumor-specific copy number imbalance. After the generation of text files in CNAG mapping arrays (which contained information on each SNP probe's identification, locus, physical position, $\log_2$ ratio, and inferred copy number), data were imported into Spotfire Decision Site, along with 100K or 500K annotation based on the NetAffx files build 11/15/09 (http://www.affymetrix.com). The X chromosome was not analyzed because of the use of both sexes in the reference sets. Chromosomal arms were defined as gained or lost if >80% of probes in an arm shared the copy number imbalance. Implementing the hidden Markov model, CNAG provides a copy number of 0–6 for each probe. Homozygous deletion was defined as a copy number of 0, loss as a copy number of 1, gain as a copy number of 3–5, and amplification as a copy number of 6. A threshold of $\geq$5 consecutive SNPs harboring the same copy number was considered to be a true alteration, and the genes in these regions were identified. Gene lists of the most common copy number gain and loss in primary and recurrent CNS PNETs and pineoblastomas were created in Spotfire and ordered by frequency. In addition, to further identify regions of interest, GISTIC analysis was performed in Genespring GX 11.2 (Agilent) for the 100K and 500K datasets of 18 and 11 primary CNS PNETs, respectively. Regions with q values <0.25 were deemed significant and were plotted in a chromosome ideogram using Photoshop, version 6.0 (Adobe). Gene lists were also created in Spotfire for the most common regions of maintained and acquired copy number alteration and were ordered by frequency. Matching regions of gain and loss identified in both the primary and recurrent tumors from the same patient were termed "maintained" alterations, whereas regions of gain and loss identified at relapse that had normal copy numbers in the primary tumor were termed "acquired" alterations. To visualize the maintained and acquired copy number alterations in 5 paired primary and recurrent CNS PNETs, the in-house tool SNPview was used.

Real-time qPCR Validation of SNP Array Data

To validate the SNP array data, candidate gene copy number alterations (including *ABCG5, ABCG8, CADPS, CDKN2A, CDKN2B, FAM129A, MYCN, OR4C12, PCDHGA3, PDGFRA,* and *SALL1)* were analyzed by quantitative PCR (qPCR) in samples with available DNA. Genes were chosen on the basis of their relationship when compared with clinical factors, such as a high frequency of abnormal gene copy number throughout the majority of samples or being situated in the most commonly maintained region of 5 primary and recurrent CNS PNET pairs. Relative gene copy number was determined by SYBR green real-time qPCR using the Mx4000 cycler (Stratagene). Primer sequences are shown in Supplementary Material, Table S1, and standard PCR cycling conditions were followed from the manufacturer's protocol (Stratagene). In addition, the copy number of 5 regions within an amplicon at 19q (coding for *miR-512*, *miR527*, *miR372*, *NLRP12,* and *LILRA4*) were investigated using previously published primer sequences.[10] All primer sets had optimal annealing temperatures of 58°C. PCR reactions were performed in triplicate for each primer set, and copy number results were determined using the Pfaffl equation, accounting for differences in primer efficiencies.[28] Tumor-specific gene copy number was confirmed by comparison of the threshold fluorescence (Ct value) for tumor DNA and constitutional DNA in both reference and candidate genes. The reference gene *ARHGAP10* (4q31.23) was used because of its normal copy number of 2 (from the SNP array data) throughout all tumor and constitutional samples.

Comparison of Copy Number Imbalance in CNS PNET and Medulloblastoma

In addition to the GISTIC analysis of 18 primary CNS PNETs (100K mapping set) and 11 primary CNS PNETs (500K mapping set), publically available SNP array data for 74 primary medulloblastomas (100K array mapping set) and 102 primary medulloblastomas (500K array mapping set) from pediatric patients (age, <16 years) were subsequently analyzed using GISTIC (GSE14437).[29] Affymetrix CEL files were imported into Genespring GX 11.2 (Agilent), and data were normalized against publically available 100K and 500K data from 270 HAPMAP samples.[27] GISTIC analysis was performed in Genespring, and regions with q values <0.25 were deemed to be significant. Regions of significant gain and loss in the CNS PNET and medulloblastoma cohorts were further explored in Excel 2007 (Microsoft), and with the use of formulae, regions of copy number imbalance specific to CNS PNET, specific to medulloblastoma, or shared between the anatomically distinct PNETs were identified.

Immunohistochemical Analysis of p15INK4b in CNS PNET and Pineoblastoma

After histopathologic review, 52 formalin-fixed paraffin-embedded (FFPE) tumor tissue blocks were available for inclusion in a tissue microarray (TMA). Thirty-three FFPE tumors had scorable results. Five were primary pineoblastomas from patients aged 5–183 months, with a mean age at diagnosis of 67.8 months. Twenty-eight CNS PNETs were included in the immunohistochemical analysis of p15INK4b expression: 22 were primary samples (taken during the patients' first surgery), and 6 were recurrent samples (taken at a later surgery due to tumor recurrence; 3 were from patients with a paired primary tumor). The age of patients with CNS PNET ranged from 6 to 149 months, with a mean age of 76.6 months. Because of their histopathological similarities[3] and similar treatment protocols in the United Kingdom,[5] both patients with pineoblastomas and those with CNS PNETs were included in the cohort. FFPE blocks and patient clinical information were collected from 2 Children's Cancer and Leukaemia Group–registered centers in the United Kingdom. Immunohistochemistry was performed as described elsewhere.[30] A 1:50 dilution of mouse monoclonal antibody for p15INK4b (15P06, ab4068-500; Abcam) was incubated overnight at 4°C. Colon carcinoma was used as a positive control. The scoring for p15INK4b protein expression consisted of the evaluation of both the percentage of positive cells and the intensity of positive staining. Tumors were scored as negative, weak, moderate, or strong for p15INK4b staining. Weak staining was considered if $<50\%$ of cells had low-intensity staining findings, moderate staining was considered if $\geq 50\%$ of cells had low-intensity staining findings, and strong staining was considered if $\geq 50\%$ of cells had intense staining findings. p14ARF and p16INK4a (encoded by *CDKN2A* and *CDKN2B*, respectively) were not assessed on the TMAs because of either withdrawal of the antibody from the market or difficulties in optimization.

Statistics

Statistical analysis was performed using SPSS software, version 16.0. To test for a significant correlation between SNP array copy number and real-time qPCR results for candidate genes validated, Spearman rank correlation was performed. The Fisher exact test was performed to investigate whether validated gene copy number alterations or p15INK4b protein expression were significantly associated with primary or recurrent tumors, tumor location (CNS PNET vs pineoblastoma), and metastatic status. With age a continuous variable, independent-sample *t* tests were performed to investigate whether copy number alterations or p15INK4b protein expression was associated with patient age. Finally, to test whether specific gene copy number imbalance or p15INK4b protein expression correlated with patient survival, univariate survival curves were constructed in SPSS using the Kaplan-Meier method, and comparisons were made using the log-rank test (Mantle-Cox).

Results

The Majority of CNS PNETs Have Complex Genomic Alterations

Thirty-six CNS PNETs and 8 pineoblastomas were analyzed using either Affymetrix 100K and 500K mapping sets (Table 1). Mean SNP call rates were 96.66% and 91.15% for the 50K Xba1 and 50K HindIII arrays, respectively, whereas the 250K NspI and 250K StyI arrays had mean SNP call rates of 96.67% and 94.08%, respectively. The raw data analyzed are available from the Gene Expression Omnibus (http://www.ncbi.nlm.nih.gov/geo/; accession number GSE12370). Copy number data were visualized in Spotfire as heat maps to identify regions of gain and loss throughout the tumor genomes. Separate heat maps are shown illustrating primary and recurrent CNS PNETs and pineoblastomas in age order (Fig. 1A and B). Overall, the majority of CNS PNETs contained a greater degree of genomic imbalance, compared with pineoblastomas. However, 3 primary and 1 recurrent CNS PNET were found to have balanced (copy number–neutral) genomes, which were later confirmed in 3 CNS PNETs (previously analyzed using the 100K SNP arrays) when reanalyzed using the higher-resolution 500K SNP arrays (data not shown). The extent of copy number imbalance in tumors increased with patient age at diagnosis. However, these observations were not statistically significant when tested using the Mann-Whitney *U* test.

Chromosome Arm Imbalance in CNS PNET and Pineoblastoma

The most common chromosome arm alterations identified in primary CNS PNETs were gains of 19p (8 [27.6%] of 29), 2p (7 [24.1%] of 29), and 1q (6 [20.7%] of 29). In recurrent CNS PNETs, 20q and 21q were the most common gains, identified in 3 (50%) of 6 cases. 16q was the most frequently lost chromosome arm, occurring in 3 (10.3%) of 29 primary CNS PNETs and 2 (33%) of 6 primary pineoblastomas. Chromosome arm imbalance was not present in the 2 recurrent pineoblastomas studied. Statistical associations linking chromosome arm imbalance and examined patient clinical characteristics were not identified.

Focal Gain of Gene Copy Number in CNS PNET and Pineoblastoma

To identify regions of copy number gain, the most common regions containing 5 consecutive SNPs from the 100K and 500K SNP array analyses were identified and ordered by frequency (Supplementary Material, Tables S2–S6). The protocadherin gene, *PCDHGA3*

Table 1. Patient clinical characteristics and chromosome arm imbalance

Tumor ID	Histology/WHO classification	Sex	Age at diagnosis, months	Primary/ recurrent	Location	Metastasis	Follow-up, months	Censor	SNP array	Gains	Losses
Pineoblastomas											
1	Pineoblastoma	F	6	P	PR	M3	10	U	100K	-	-
2	Pineoblastoma	M	12	P	PR				100K	19p	16q
3	Pineoblastoma	F	13	P	PR	M3	10	U	100K	1q, 6p	16q
4	Pineoblastoma	M	15	R	PR	M3	20	U	100K	-	-
5	Pineoblastoma	M	24	P	PR	M0	179	C	100K	-	-
6	Pineoblastoma	M	24	R	PR				100K	-	-
7	Pineoblastoma	M	132	P	PR				100K	-	-
8	Pineoblastoma	F	168	P	PR				100K	-	-
CNS PNETs											
9	CNS PNET	F	10	P	CR - Pa	M2	41	U	100K	-	-
10[a]	CNS PNET	F	10	R to 9	CR - Fr	M2	41	U	100K and 500K	-	-
11	CNS PNET	F	14	P	CR	M1	24	C	500K	19p, 19q	-
12	CNS PNET	M	19	P	CR, PF	M3	11	U	100K	-	-
13	CNS PNET	M	19	P	CR - Fr, T	M0	20	U	100K	1q, 19p	16q
14[a]	CNS PNET	M	19	R to 13	CR - Fr, T	M0	20	U	100K	1q, 2q, 12p, 16p, 20q, 21q	-
15[a]	CNS PNET	F	20	P	CR - Fr	M0	0	U	100K and 500K	-	-
16	CNS PNET cell line	M	22	P	CR				500K	1q, 2p, 7p, 8p, 8q, 11p, 19p, 19q, 21q	-
17	CNS PNET	F	23	P	CR - T	M0	7	U	500K	-	17p
18[a]	CNS PNET	F	24	P	CR - T	M0	3	U	100K	19p	-
19	CNS PNET with true rosettes	F	26	P	CR	M0	3	U	500K	2p, 2q	-
20	CNS PNET	M	32	P	CR - Fr				100K	2p[b], 17p, 19p	2q[b]
21	CNS PNET	F	36	P	CR - T, Pa	M0	16	U	500K	-	-
22[a]	CNS PNET	M	37	P	CR - T	M4	6	U	100K	2p, 2q, 8p, 11q, 12p, 12q, 13q[c], 20p, 20q	-
23	CNS PNET	F	51	P	CR - T, Pa	M0	24	U	100K and 500K	-	-
24[a]	CNS PNET	F	53	P	CR - T, Pa	M0	22	C	100K	1q, 17p, 17q, 18p, 18q	16q
25[a]	Cerebral neuroblastoma	M	59	P	CR - Mi, Fr	M2	9	U	100K	7p, 17p, 17q, 19p, 19q	9p
26[a]	CNS PNET	M	61	P	CR - Fr	M0	21	U	100K	2p	-
27	CNS PNET	M	61	P	CR - T	M0	2	U	500K	1q	-
28	CNS PNET	F	71	P	CR - Fr, Pa	M0	5	U	100K	17p, 17q, 22q	3p, 6q, 16q
29	CNS PNET	M	77	P	CR - T	M0	17	U	500K	1q, 2p, 7p, 7q, 16p, 16q, 18p, 20p, 20q, 21q[c]	-

30	CNS PNET	M	84	P	CR - P	M1	20	U	500K	5p, 5q, 8p, 8q, 16p, 16q, 20p, 20q, 21q	-
31[a]	CNS PNET	F	85	P	CR - Fr	M0	83	C	100K	1q[c], 2p, 2q, 7p, 7q, 18p, 19p, 21q, 22q	-
32	CNS PNET	F	91	P	CR - Fr	M1	31	C	500K	19p, 19q	-
33[a]	CNS PNET	M	107	P	CR	M2	71	U	100K	2p, 2q, 12p, 12q	-
34[a]	CNS PNET	M	107	R to 33	CR, PF	M2	71	U	100K	1q, 3q, 5p, 8p, 8q, 9p, 9q, 10p, 16p, 17q, 19p, 19q, 20p, 20q, 21q, 22q	5q
35[a]	CNS PNET	M	122	P	CR - Pa	M0	52	C	100K	-	-
36[a]	CNS PNET	M	122	R to 35	CR - Pa	M0	52	C	100K	12p, 12q, 13q, 20q	-
37	CNS PNET	M	127	P	CR - Pa	M0	27	C	500K	1q, 3q, 5p, 5q, 8p, 8q, 13q, 21q	-
38	CNS PNET	M	141	P	CR - Fr	M3	30	U	100K	-	9p, 9q
39	CNS PNET	M	141	R to 38	CR - Fr	M3	30	U	100K	17p, 18p, 21q	-
40[a]	CNS PNET	M	142	P	CR - H, LV	M0	0	U	100K	5p, 5q, 19p, 19q	-
41	CNS PNET	F	144	P	CR	M0	3	C	500K	4q, 20p, 20q	-
42[a]	CNS PNET	F	148	R	CR - Fr, Pa		36	U	100K	17p	-
43	CNS PNET	F	190	P	CR	M0	15	C	500K	-	-
44	CNS PNET	M		P	CR - Pa				100K	2q, 7p, 7q, 11p, 11q, 12p, 12q, 20p, 21q	-

Patient clinical information was collected along with the 8 pineoblastomas and 36 central nervous system primitive neuroectodermal tumor (CNS PNET) samples analyzed on the Affymetrix single nucleotide polymorphism arrays.

Abbreviations: C, censored (alive); CR, cerebral region; Fr, frontal lobe; F, female; H, hemispheric; LV, lateral ventricle; M, male; Mi, midline; P, primary; Pa, parietal; PF, posterior fossa; PR, pineal region; R, recurrence; T, temporal lobe; U, uncensored (deceased); WHO, World Health Organization - indicates no alteration was identified. Information was not available for boxes left blank.

[a]Sample was included in immunohistochemical study.

[b]Isochromosome.

[c]High-level gain. Metastatic status was based on Chang staging M0–M4.

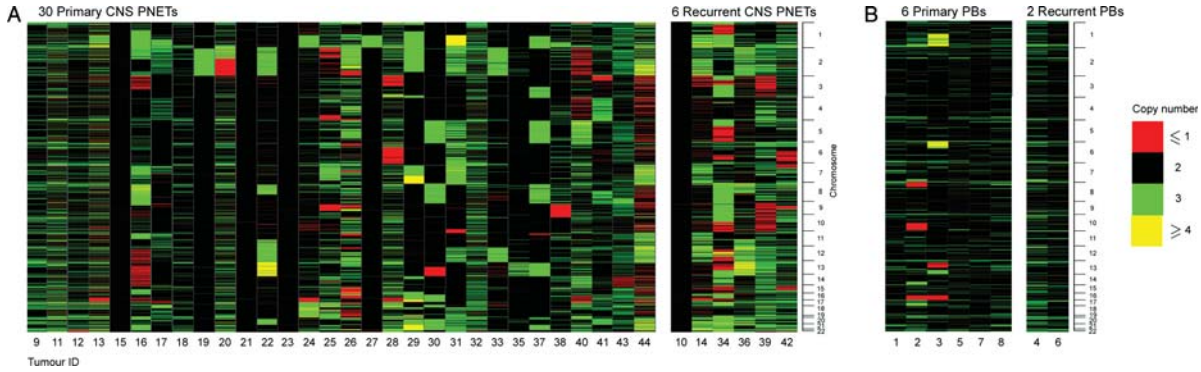

Fig. 1. Heat map visualization of the genome-wide copy number results for (A) 30 primary and 6 recurrent central nervous system primitive neuroectodermal tumors (CNS PNETs) and (B) 6 primary and 2 recurrent pineoblastomas (PBs) using Affymetrix 100K and 500K single nucleotide polymorphism arrays. Heat maps were generated using Spotfire. Tumor heat maps are in age order, increasing from left to right. Copy number results are shown for chromosomes 1–22 from top to bottom. Red, copy number loss; black, copy number neutral; green, copy number gain; yellow, high-level gain (copy number ≥4). Each column represents a single tumor sample.

(5q31.3), was frequently gained, occurring in 18 (62.1%) of 29 primary CNS PNETs, in addition to 4 (66.7%) of 6 recurrent CNS PNETs, 6 (100%) of 6 primary pineoblastomas, and 2 (100%) of 2 recurrent pineoblastomas. *FAM129A* (1q25.3) was found to be gained frequently, occurring in 5 (83.3%) of 6 recurrent CNS PNETs, in addition to 16 (55.2%) of 29 primary CNS PNETs and 3 (50%) of 6 primary pineoblastomas. Gain of *FAM129A* was not found in the 2 recurrent pineoblastomas studied. GISTIC analysis of the 100K and 500K datasets further supported the gain of these genes to potentially have a role in the pathogenesis of CNS PNET (Supplementary Material, Figs S1 and S2). The identified increases in gene copy number were validated by real-time qPCR (Supplementary Material, Fig. S3). A statistical comparison of the copy numbers of gained and lost genes identified from the SNP array analysis, validated by real-time PCR, revealed a positive correlation between the 2 sets of copy number results, demonstrating the SNP array copy number data to be both accurate and reliable ($r = 0.831$, significant at the 0.01 level [2-tailed]).

Amplification of MYCN *and* PDGFRA *in CNS PNET*

Thirty-two distinct regions of amplification (based on the maximum copy number given by CNAG analysis of 6) were identified, including 2p24.3, which encompasses the proto-oncogene *MYCN* in CNS PNET 25 (a cerebral neuroblastoma) and 4q12, which encompasses *PDGFRA* in a recurrent tumor, CNS PNET 34 (Supplementary Material, Table S7).

19q13.41 Amplification in a CNS PNET with Variant Histology

Because of the recent discovery of an amplified miRNA cluster (*C19MC*) encompassing 19q13.41 in CNS PNETs with variant histology, this region was examined in detail. We identified 19q13.41 amplicon in 1 (3.4%) of 29 primary CNS PNETs and validated the result using real-time qPCR, to reveal >9 copies of the DNA sequence coding for miRNA's miR-512, -527, and -372 (Fig. 2A–D). In addition to the 19q13.41 amplicon, CNS PNET 19 also had gain of chromosome 2, and under histological examination, true rosettes were observed.

Focal Loss of Gene Copy Number in CNS PNET and Pineoblastoma

To identify common gene copy number losses in 35 CNS PNETs and 8 pineoblastomas, the most frequently lost genes from the 100K and 500K SNP array analyses were identified and ordered by frequency (Supplementary Material, Tables S8–S12). *OR4C12*, encoding an olfactory receptor on 11p11.12, was lost in 14 (48.3%) of 29 primary CNS PNETs, in addition to 3 (50%) of 6 recurrent CNS PNETs and 3 (50%) of 6 primary pineoblastomas. *OR4C12* loss was not found in the 2 recurrent pineoblastomas studied. Gene copy number loss also frequently involved *CADPS* (3p14.2), occurring in 8 (27.6%) of 29 primary CNS PNETs and 4 (66.7%) of 6 recurrent CNS PNETs. This alteration was only identified in 1 (16.7%) of 6 primary pineoblastomas and 0 of the 2 recurrent pineoblastomas. Homozygous deletions in the tumor cohort were also identified (Supplementary Material, Table S13). A large region of 9p21.3 was homozygously lost in 4 CNS PNETs (Fig. 3). The loss encompassed genes *MTAP*, *CDKN2A*, *CDKN2B,* and *DMRTA1* in 3 tumors (CNS PNET 25, in addition to the paired primary and recurrent CNS PNETs 38 and 39), whereas a fourth tumor had homozygous loss involving only *MTAP*, *CDKN2A*, and *CDKN2B* (CNS PNET 29). Loss of *CDKN2A/B* was observed only in CNS PNETs (4 [13.8%] of 29 primary CNS PNETs, 3 [50%] of 6 recurrent CNS PNETs, and 0 of 8 pineoblastomas) from children aged ≥4 years, 11 months. However, in this small subset of tumors, a

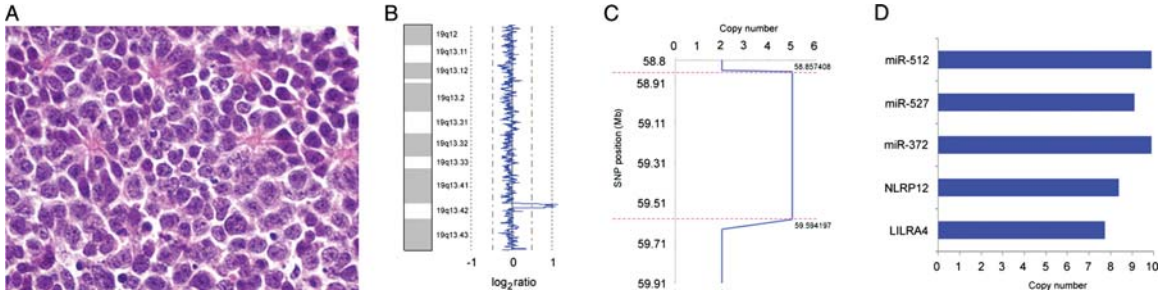

Fig. 2. 19q13.41 amplification of *C19MC* miRNAs. (A) Histopathologic examination of central nervous system primitive neuroectodermal tumor (CNS PNET) 19 showed a primitive embryonal tumor with true rosettes. (B) Amplification at 19q13.41 was identified in this case, with (C) the 0.73 Mb amplicon spanning 58.85–59.59 Mb. (D) Real-time quantitative polymerase chain reaction of miRNAs and genes in this region validated the amplification in copy number.

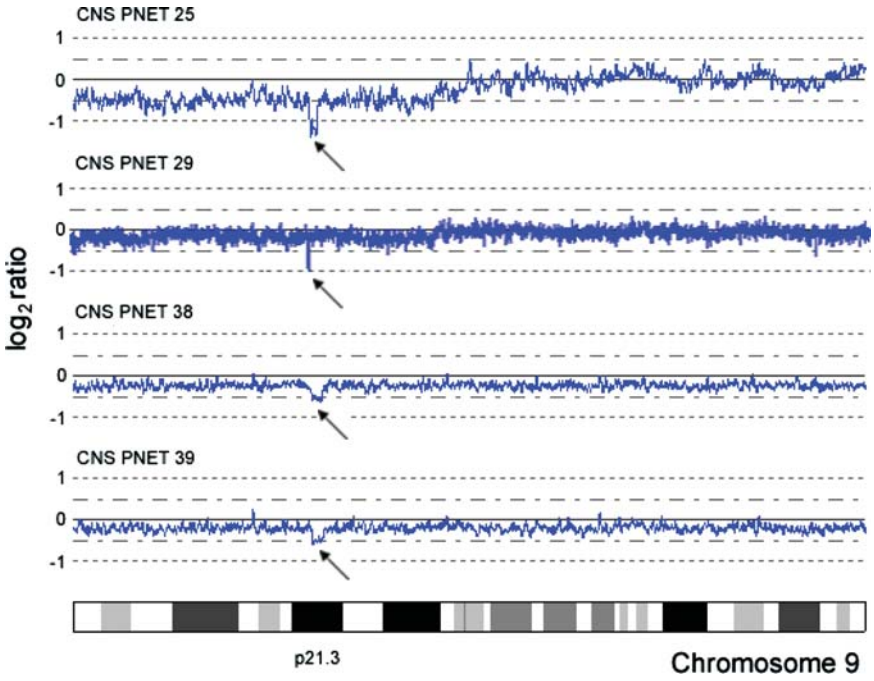

Fig. 3. Homozygous loss at the 9p21.3 locus. Homozygous loss at loci 9p21.3 encompassing *CDKN2A* and *CDKN2B* was identified in 4 cases (arrows). Of the tumors with homozygous loss at 9p21.3, central nervous system primitive neuroectodermal tumor (CNS PNET) 29 retained both copies of chromosome 9, CNS PNET 25 had biallelic loss of chromosome 9p, and CNS PNETs 38 and 39 (a paired primary and recurrence of the same patient) had lost 1 copy of the entire chromosome.

statistically significant result was not identified. A mutational screen of *CDKN2A* and *CDKN2B* in 30 tumors that either had normal DNA copy number or had loss of 1 allele did not reveal mutations affecting coding regions (data not shown).

GISTIC analysis of the 100K and 500K datasets further supported a potentially important role for the loss of these genes in the pathogenesis of CNS PNET (Supplementary Material, Figs S1 and S2). Gene copy number loss identified was validated by real-time qPCR (Supplementary Material, Fig. S4). Statistical analysis was performed using appropriate tests to identify whether genes chosen for real-time qPCR (*PCDHGA3*, *FAM129A*, *MYCN*, *PDGFRA*, *OR4C12*, *CADPS*, *CDKN2A*, *CDKN2B*, and *SALL1*) were significantly associated with clinical parameters (patient age, tumor location, metastatic status, tumor recurrence, and patient survival). A single significant result was identified: loss of *CADPS* was associated with a poorer prognosis (Supplementary Material, Fig. S5).

Comparison of Paired Primary and Recurrent CNS PNETs Revealed Both Regions of Maintained and Acquired Copy Number Alteration at Relapse

Genome-wide copy number analysis of 5 paired primary and recurrent CNS PNETs was performed, identifying regions of maintained copy number (Fig. 4). Large regions of gain on chromosome 1q were identified in primary CNS PNET 13 and were maintained at relapse

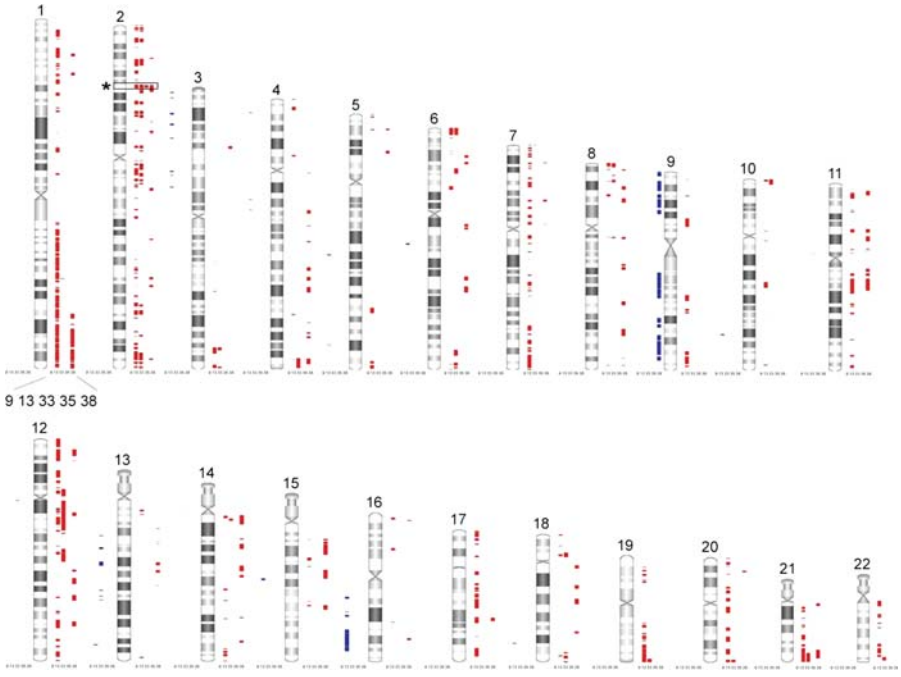

Fig. 4. Regions of maintained gain and loss identified in 5 paired primary and recurrent central nervous system primitive neuroectodermal tumors (CNS PNETs). Shown is a chromosome ideogram of the maintained copy number imbalance in 5 paired primary and recurrent CNS PNETs analyzed using Affymetrix 100K single nucleotide polymorphism arrays. Visualization was made in SNPview. Maintained loss is shown to the left of the chromosome (blue), and maintained gain is shown to the right (red). 2p21 (starred) was the most common region of maintained gain, occurring in 4 (80%) of 5 CNS PNET pairs.

(paired recurrent CNS PNET 14). Gain of 13q was found in primary CNS PNET 35, with this alteration maintained at recurrence (CNS PNET 36). To identify the most common regions of maintained gene copy number alteration, the most frequently altered regions shared between the 5 tumor pairs were identified from the 100K SNP array analyses and ordered by frequency (Supplementary Material, Tables S14 and S15). Regions of maintained gain were observed more frequently than regions of loss. The most commonly maintained regions of alteration involved focal gains on chromosome 2, particularly at 2p21 (in 4 [80%] of 5 CNS PNET pairs). Encompassing *ABCG5* and *ABCG8*, the maintained gain at 2p21 was validated in the primary and recurrent CNS PNET pairs using real-time qPCR (Supplementary Material, Fig. S6). Regions of maintained loss were identified, most frequently involving 9p24.1 and 9q33.1 (2 [40%] of 5 CNS PNET pairs). Maintained loss of large regions on 3p, 5q, and 9p (encompassing *CDKN2A/B*) and on 9q, 13q, and 16q (in 1 [20%] of 4 CNS PNET pairs) were also identified.

An overview of the acquired copy number alterations is shown in Supplementary Material, Fig. S7. To identify the most common regions of acquired gene copy number alteration, the most frequently altered regions found at recurrence (not observed in the paired primary tumors) were identified from the 100K SNP array analyses and ordered by frequency (Supplementary Material, Tables S16 and S17). The acquired regions of alteration at relapse potentially encompass genes involved in tumor progression and relapse; however, because of treatment-induced genomic instability of the tumor's genome, it is hard to decipher "true" tumorigenic events from those of therapy-related genomic instability. One recurrent tumor (CNS PNET 34) was found to have 2 novel regions of amplification at 4q12 and 12q14.1 that were not present in the primary tumor (CNS PNET 33; Fig. 5). The high-level gain identified at 4q12 encompassed *PDGFRA*, encoding a cell-surface tyrosine kinase receptor for the platelet-derived growth factor family of mitogens, in addition to the co-amplification of the proto-oncogene *c-KIT* (*KIT*), whereas the high-level gain at 12q14.1 encompassed the genes *GLI1* and *CDK4*.

Comprehensive Comparative Analysis of Genomic Alterations in CNS PNET and Medulloblastoma Revealed Both Tumor-Specific and Shared Regions of Imbalance

Significant regions of CNS PNET–specific gain were found throughout the genome, including the gain of *PCDHGA3* (Supplementary Material, Table S18 and S19). Fewer regions of medulloblastoma-specific gain were identified, limited to 1q, 2p, 4p16, 4q, and 5 and to many regions of chr 7, 9p, 8q, 14q, 17, 18, and 19q (Supplementary Material, Tables S20 and S21). Significant regions shared between both PNETs included 1q (1q42 – 44), 2p25.3-1 encompassing *MYCN*, 4p16, 7 (7q36), 17q, and 18q (Supplementary Material, Tables

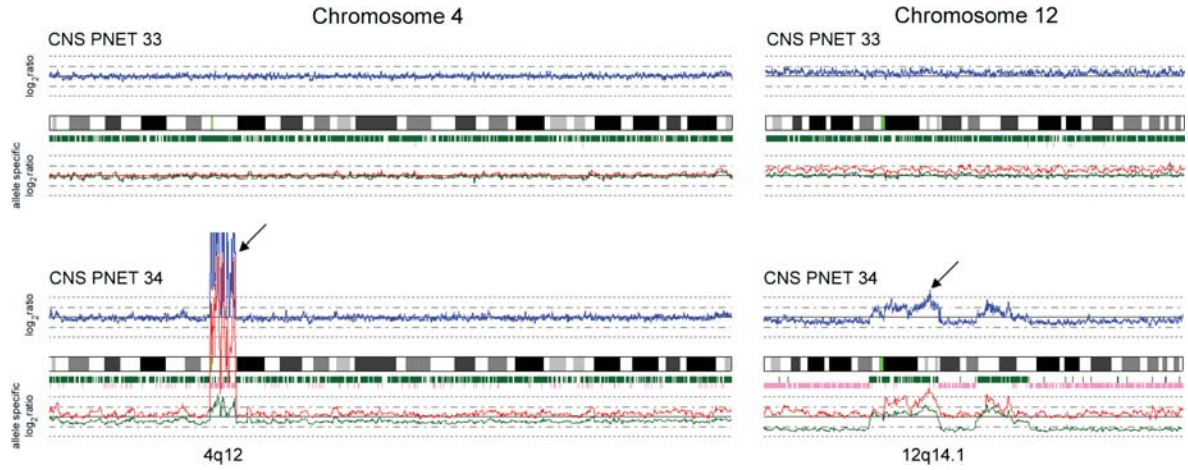

Fig. 5. Two distinct regions of amplification identified in a recurrent central nervous system primitive neuroectodermal tumor (CNS PNET) that were not present in the primary tumor of the same patient. Although the recurrent tumor (CNS PNET 34) had amplifications at 4q12 and 12q14.1, this was not observed in the primary tumor (CNS PNET 33). Data were visualized in Copy Number Analyzer for Affymetrix Genechip. Green bars indicate heterozygous single nucleotide polymorphism calls and pink bars indicate loss of heterozygosity.

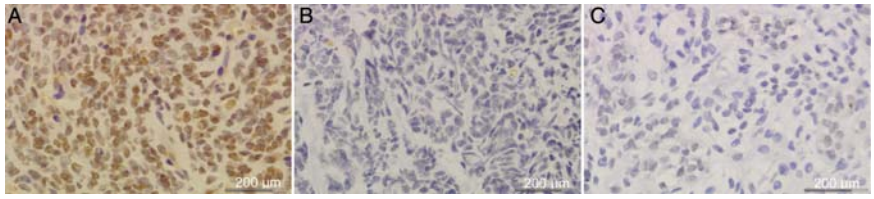

Fig. 6. Immunohistochemical evaluation of p15INK4b protein expression. (A) Central nervous system primitive neuroectodermal tumor (CNS PNET) 35 retained both copies of *CDKN2B* and displayed strong positive protein expression for the encoded protein, p15INK4b. (B) CNS PNET 40 also retained both allele copies of the *CDKN2B* gene; however, it showed no protein expression for p15INK4b. (C) CNS PNET 36 had a single allele present due to the loss of 1 copy of *CDKN2B* and showed the absence of p15INK4b protein expression.

S22 and S23). CNS PNET–specific deletion was found on focal regions of 2p and 2q, large regions of chromosome 3 (encompassing *CADPS*), 4q, 9p (including *CDKN2A* and *CDKN2B*), 14q, and 15q (Supplementary Material, Tables S24 and S25). There were many regions of medulloblastoma-specific deletion that included large regions of chromosome 6, 10, 11, and 16 (Supplementary Material, Tables S26 and S27). Both PNET cohorts shared significant regions of deletion involving chromosomes 10q, 11 (encompassing *OR4C12*), and 16q (Supplementary Material, Tables S28 and S29).

Immunohistochemistry of CDKN2B *(p15INK4b)*

To determine whether loss of *CDKN2B* gene copy number (identified using the SNP array analysis in 7 [16.3%] of 16 cases in the tumor cohort) affected the level of expression for the encoded protein (p15INK4b), we performed immunohistochemistry on 28 CNS PNETs and 5 pineoblastomas (Fig. 6). Fifteen were tumors that had been analyzed using the SNP array sets (as shown in Table 1), whereas an additional 18 FFPE samples were available for inclusion in a TMA. Eight (24.2%) of 33 tumors had negative p15INK4b staining results (6 were primary CNS PNETs, 1 was a recurrent CNS PNET, and 1 was a primary pineoblastoma). Protein expression was compared with *CDKN2B* array data where available. Three tumors negative for p15INK4b staining had corresponding SNP array copy number data for *CDKN2B*. Two tumors had homozygous loss of *CDKN2B*, whereas the third p15INK4b-negative tumor had retained both copies. Six (18.2%) of 33 tumors had weak staining findings (4 were primary CNS PNETs, 1 was a recurrent CNS PNET, and 1 was a primary pineoblastoma). Two tumors with weak p15INK4b staining had normal gene copy numbers. Eight (24.2%) of 33 tumors had moderate staining findings for p15INK4b (4 were primary CNS PNETs, 2 were recurrent CNS PNETs, and 2 were primary pineoblastomas), of which 3 had a normal copy number for *CDKN2B* and 1 tumor had lost a single copy. Finally, 11 (33.3%) of 33 tumors had strong staining findings for p15INK4b (8 were primary CNS PNETs, 2 were recurrent CNS PNETs, and 1 was a primary pineoblastoma). Four strongly staining tumors had a normal gene copy number, 1 had a gain in *CDKN2B* copy number, and 1 tumor had lost 1 allele copy. Statistical comparisons between p15INK4b immunohistochemical staining findings and patient clinical demographic characteristics were performed. Using the

the Fisher exact test, a single trend was identified that suggested strong p15INK4b protein expression was associated with patients without metastatic disease at diagnosis ($P = .055$ for primary CNS PNET).

Discussion

This high-resolution genome-wide analysis showed that tumors classified histologically as CNS PNET show considerable heterogenity at the molecular level. Marked differences were seen in the genomic profiles on the basis of anatomical location and patient age, with the majority of CNS PNETs characterized by multiple genetic alterations, compared with relatively few copy number alterations in pineoblastoma. The differential genomic profiles may reflect distinct origins of these tumors, as seen for other CNS tumors.[31,32] Novel candidate genes potentially involved in the pathogenesis of CNS PNET and pineoblastoma were identified and confirmed by GISTIC analysis. Gain of *PCDHGA3* (5q31.3) and *FAM129A* (1q25.3) were common gains identified in the tumor cohort. Encoding a neural cadherin-like cell adhesion protein, *PCDHGA3* (protocadherin gamma subfamily A3) has potential roles in the establishment and function of cell-to-cell connections in the brain, whereas *FAM129A* regulates the phosphorylation of a number of proteins involved in translation regulation. Loss of *CADPS* (3p14.2), which encodes a calcium-binding protein involved in exocytosis of vesicles filled with neurotransmitters and neuropeptides, was identified in the CNS PNET cohort and was associated with a poor prognosis ($P = .043$). Confirmation of the loss of *CADPS* and its impact on patient survival is now needed in a larger cohort of CNS PNETs to corroborate our findings from this relatively small sample set.

Gain of chromosome 2 was found in primary CNS PNETs (2p gained in 7 [24.1%] of 29, and 2q gained in 5 [17.2%] of 29 primary CNS PNETs) and has been shown to be a feature in other genetic studies of CNS PNET.[7,10,21] Moreover, the comparison of 5 paired primary and recurrent CNS PNETs showed that the most frequent region of maintained gain involved genes on 2p21 in 4 (80%) of 5 CNS PNET pairs. Interestingly, *ABCG5* and *ABCG8* are encompassed within this locus, with ATP-binding cassette transporters thought to have an involvement in the multidrug resistance of brain tumor therapies.[33] These data suggest that oncogenes involved in both initiating and sustaining CNS PNET pathogenesis are located on chromosome 2p and warrant further investigation.

19q13.41 amplification (encompassing *C19MC*) has been associated with a spectrum of CNS PNET histologies and identifies a subgroup of highly aggressive PNETs of poor prognosis.[10,34–36] The amplicon has predominantly been found in the so-called "CNS PNET variant"; gain of chromosome 2, ependymal/ependymoblastic differentiation, and/or true rosettes are distinguishing features.[10,34,35] However, ~10% of CNS PNETs with "classic" histology have also been observed to harbor this amplification.[10] The majority of CNS PNETs (97.1%) in our study had "classic" histology, depicted by small, blue, round cells with little or no differentiation. We found only 1 (3.4%) of 29 primary CNS PNETs with amplification of *C19MC*. Li et al[10] reported the 19q13.41 amplification in 24% of their study cohort cases. The variation in frequency of *C19MC* amplification likely reflects the heterogeneous nature of CNS PNETs and emphasizes the need to increase the sample set of biological data in this tumor.

The cyclin-dependent kinase inhibitors *CDKN2A* and *CDKN2B* (9p21.3) are frequently lost in a wide range of pediatric malignancies, including brain tumors.[8,9,37–41] p16INK4a and p15INK4b (encoded by *CDKN2A* and *CDKN2B*, respectively) can induce cell-cycle arrest at both G1 and G2/M checkpoints. Loss of function results in deregulation of normal cellular proliferation, resulting in unchecked growth.[42] *CDKN2A* and *CDKN2B* gene copy number loss was identified in 13.8% of primary CNS PNET cases and has also been observed in other series.[8,9] In our cohort, 9p21.3 deletions were only found in patients with CNS PNET aged >4 years. Although this result was not significant for our results alone, the compilation of our results for *CDKN2A/B* with those of a previous genetic study[9] revealed a statistically significant result: the loss of *CDKN2A/B* is age dependent in primary CNS PNETs ($P = .05$, by Mann-Whitney U test; S. Pfister, personal communication). We previously reported differential loss of *CDKN2A/B* in high-grade gliomas on the basis of the anatomical location of the tumor reporting deletions of these genes in supratentorial high-grade glioma, but not in diffuse intrinsic pontine glioma, consistent with a cell of origin event.[43] In a recent article by Pfister et al,[9] the comparison of aCGH profiles for CNS PNETs and medulloblastomas also revealed that the loss of *CDKN2A* was significantly associated with CNS PNETs ($P < .001$). None of the pineoblastomas in the present cohort had the deletion. Comparison of CNS PNET and medulloblastoma gene lists identified using GISTIC found that the loss of *CDKN2A* and *CDKN2B* was a CNS PNET–specific event. Taken together, these results suggest that different pathways are involved in the development of CNS PNET, medulloblastoma, and pineoblastoma. We extended our analysis to investigate the loss of expression of p15INK4b (encoded by *CDKN2B*) and demonstrated loss in 24.2% of tumors. Two tumors with weak p15INK4b staining had normal *CDKN2B* gene copy numbers. Taken together, these results suggest mechanisms other than *CDKN2B* copy number loss to be involved in the loss of p15INK4b protein expression. In 2007, Pfister et al[9] identified a trend with *CDKN2A* deletion and metastasis in CNS PNET ($P = .07$). This statistical link was upheld on the compilation of our SNP array dataset with these previous aCGH and FISH results ($P = .07$). Furthermore, we identified an association with strong p15INK4b staining in primary CNS PNETs without metastatic disease at diagnosis. Collectively, this evidence highlights a potential role for the loss of *CDKN2A/*

CDKN2B in the development and progression of a subset of CNS PNETs.

The extent of chromosome arm alteration across the genome was noted to be higher in the CNS PNETs arising in children aged ≥3 years versus those arising in children aged <3 years. Pineoblastomas were also characterized by relatively few imbalances, compared with supratentorial CNS PNETs. The observed differences in the extent of copy number change between CNS PNETs and pineoblastomas may reflect differences in the cells of origin for these primitive embryonal neoplasms, as was shown in ependymoma.[44] Alternatively, this finding might reflect a combination of the differences in patient age and tumor location, because pineoblastomas usually occur in younger children, who, in turn, tend to have fewer genomic alterations.

Of note, 3 primary CNS PNETs and 1 recurrent CNS PNET were found to have copy number neutral genomes when analyzed using 100K and, subsequently, 500K SNP array platforms. Because tumor content was carefully checked (≥90%), this suggests mechanisms other than aberrant DNA copy number are an important feature in both the initiation and progression of these tumors. Other series have also reported a small number of CNS PNETs with balanced profiles.[9,10] These findings are in accordance with the hypothesis that CNS PNETs arising in very young children are biologically distinct from those occurring in older children, with fewer genetic events needed to initiate malignant change.[45,46] Additional studies to identify the molecular mechanisms of tumorigenesis in this subset of CNS PNETs, such as epigenetic changes, are needed.

Our data add to current evidence that CNS PNETs and pineoblastomas are genetically distinct from medulloblastoma. For example, isochromosome 17q, which is found in more than one-third of medulloblastomas, was not identified in our CNS PNET and pineoblastoma cohort.[7,38,47–49] Monosomy of chromosome 6 has been reported in a subset of medulloblastomas; however, none of the CNS PNETs or pineoblastomas in this study showed loss of chromosome 6.[50,51] The comparison of primary CNS PNET and medulloblastoma GISTIC lists further supported this finding, with large regions of medulloblastoma-specific loss on chromosome 6. Amplifications of *MYC* (8q24) and *MYCN* (2p24.3) have been detected in 5%–10% of medulloblastomas and are associated with poor prognosis.[38,52–54] Although only a single *MYCN* amplification was identified in the present study of CNS PNETs (2.3%), the comparison of CNS PNET and medulloblastoma GISTIC lists revealed 4p16 (encompassing *MYCN*) as a significant region of amplification shared between both infratentorial and supratentorial PNETs.

This high-resolution genome-wide analysis of a large CNS PNET and pineoblastoma cohort identified a panel of the most common genomic imbalances and novel genes potentially involved in tumorigenesis that now warrant further investigation. Although we add a considerable amount of new data, building up a comprehensive pattern of genomic change in this relatively uncommon and complex cancer will require a larger sample set. Particular effort now needs to be made to examine the gene expression and methylation profiles of these tumors, to give the results shown here greater power. To take these findings forward, collaborative efforts need to be made to bring together a large CNS PNET sample set with clinical, genetic, and histopathologic data to facilitate a greater clinical and molecular understanding of this heterogeneous and difficult-to-treat disease.

Supplementary Material

Supplementary material is available online at *Neuro-Oncology* (http://neuro-oncology.oxfordjournals.org/).

Acknowledgments

This study was a Children's Cancer and Leukaemia Group biological study. The authors wish to acknowledge Dr Lisa Storer and Sarah Leigh-Nicholson for sample collection, Lee Ridley for TMA construction, Dr Emma Prebble for assisting with the SNP array assays, and Dr Alain Pitiot and Francois Morvillier for developing SNPview.

Conflict of interest statement. None declared.

Funding

The Samantha Dickson Brain Tumour Trust (grant no. 17/53).

References

1. Dirks PB, Harris L, Hoffman HJ, Humphreys RP, Drake JM, Rutka JT. Supratentorial primitive neuroectodermal tumors in children. *J Neurooncol*. 1996;29:75–84.
2. Timmermann B, Kortmann RD, Kuhl J, et al. Role of radiotherapy in the treatment of supratentorial primitive neuroectodermal tumors in childhood: results of the prospective German brain tumor trials HIT 88/89 and 91. *J Clin Oncol*. 2002;20:842–849.
3. Louis DN, Ohgaki H, Wiestler O, Cavenee W. WHO Classification of Tumours of the Central Nervous System. 4th ed. Lyon: IARC; 2007.
4. Cohen BH, Zeltzer PM, Boyett JM, et al. Prognostic factors and treatment results for supratentorial primitive neuroectodermal tumors in children using radiation and chemotherapy: a Childrens Cancer Group randomized trial. *J Clin Oncol*. 1995;13:1687–1696.
5. Pizer BL, Weston CL, Robinson KJ, et al. Analysis of patients with supratentorial primitive neuro-ectodermal tumours entered into the SIOP/UKCCSG PNET 3 study. *Eur J Cancer*. 2006;42:1120–1128.

6. Sung KW, Yoo KH, Cho EJ, et al. High-dose chemotherapy and autologous stem cell rescue in children with newly diagnosed high-risk or relapsed medulloblastoma or supratentorial primitive neuroectodermal tumor. *Pediatr Blood Cancer*. 2007;48:408–415.
7. Inda MM, Perot C, Guillaud-Bataille M, et al. Genetic heterogeneity in supratentorial and infratentorial primitive neuroectodermal tumours of the central nervous system. *Histopathology*. 2005;47:631–637.
8. McCabe MG, Ichimura K, Liu L, et al. High-resolution array-based comparative genomic hybridization of medulloblastomas and supratentorial primitive neuroectodermal tumors. *J Neuropathol Exp Neurol*. 2006;65:549–561.
9. Pfister S, Remke M, Toedt G, et al. Supratentorial primitive neuroectodermal tumors of the central nervous system frequently harbor deletions of the CDKN2A locus and other genomic aberrations distinct from medulloblastomas. *Genes Chromosomes Cancer*. 2007;46:839–851.
10. Li M, Lee KF, Lu Y, et al. Frequent amplification of a chr19q13.41 microRNA polycistron in aggressive primitive neuroectodermal brain tumors. *Cancer Cell*. 2009;16:533–546.
11. Rogers HA, Miller S, Lowe J, Brundler MA, Coyle B, Grundy RG. An investigation of WNT pathway activation and association with survival in central nervous system primitive neuroectodermal tumours (CNS PNET). *Br J Cancer*. 2009;100:1292–1302.
12. Batanian JR, Havlioglu N, Huang Y, Gadre B. Unusual aberration involving the short arm of chromosome 11 in an 8-month-old patient with a supratentorial primitive neuroectodermal tumor. *Cancer Genet Cytogenet*. 2003;141:143–147.
13. Bayani J, Zielenska M, Marrano P, et al. Molecular cytogenetic analysis of medulloblastomas and supratentorial primitive neuroectodermal tumors by using conventional banding, comparative genomic hybridization, and spectral karyotyping. *J Neurosurg*. 2000;93:437–448.
14. Bhattacharjee MB, Armstrong DD, Vogel H, Cooley LD. Cytogenetic analysis of 120 primary pediatric brain tumors and literature review. *Cancer Genet Cytogenet*. 1997;97:39–53.
15. Bigner SH, McLendon RE, Fuchs H, McKeever PE, Friedman HS. Chromosomal characteristics of childhood brain tumors. *Cancer Genet Cytogenet*. 1997;97:125–134.
16. Brown AE, Leibundgut K, Niggli FK, Betts DR. Cytogenetics of pineoblastoma: four new cases and a literature review. *Cancer Genet Cytogenet*. 2006;170:175–179.
17. Burnett ME, White EC, Sih S, von Haken MS, Cogen PH. Chromosome arm 17p deletion analysis reveals molecular genetic heterogeneity in supratentorial and infratentorial primitive neuroectodermal tumors of the central nervous system. *Cancer Genet Cytogenet*. 1997;97:25–31.
18. Roberts P, Chumas PD, Picton S, Bridges L, Livingstone JH, Sheridan E. A review of the cytogenetics of 58 pediatric brain tumors. *Cancer Genet Cytogenet*. 2001;131:1–12.
19. Sreekantaiah C, Jockin H, Brecher ML, Sandberg AA. Interstitial deletion of chromosome 11q in a pineoblastoma. *Cancer Genet Cytogenet*. 1989;39:125–131.
20. Uematsu Y, Takehara R, Shimizu M, Tanaka Y, Itakura T, Komai N. Pleomorphic primitive neuroectodermal tumor with glial and neuronal differentiation: clinical, pathological, cultural, and chromosomal analysis of a case. *J Neurooncol*. 2002;59:71–79.
21. Avet-Loiseau H, Venuat AM, Terrier-Lacombe MJ, Lellouch-Tubiana A, Zerah M, Vassal G. Comparative genomic hybridization detects many recurrent imbalances in central nervous system primitive neuroectodermal tumours in children. *Br J Cancer*. 1999;79:1843–1847.
22. Nicholson JC, Ross FM, Kohler JA, Ellison DW. Comparative genomic hybridization and histological variation in primitive neuroectodermal tumours. *Br J Cancer*. 1999;80:1322–1331.
23. Rickert CH, Simon R, Bergmann M, Dockhorn-Dworniczak B, Paulus W. Comparative genomic hybridization in pineal parenchymal tumors. *Genes Chromosomes Cancer*. 2001;30:99–104.
24. Affymetrix. Genechip Mapping 100K Assay Protocol. Santa Clara, USA: Affymetrix.
25. Affymetrix. Genechip Mapping 500K Assay Protocol. Santa Clara, USA: Affymetrix.
26. Nannya Y, Sanada M, Nakazaki K, et al. A robust algorithm for copy number detection using high-density oligonucleotide single nucleotide polymorphism genotyping arrays. *Cancer Res*. 2005;65:6071–6079.
27. The International HapMap Project. *Nature*. 2003;426:789–796.
28. Pfaffl MW. A new mathematical model for relative quantification in real-time RT-PCR. *Nucleic Acids Res*. 2001;29:e45.
29. Northcott PA, Nakahara Y, Wu X, et al. Multiple recurrent genetic events converge on control of histone lysine methylation in medulloblastoma. *Nat Genet*. 2009;41:465–472.
30. Ridley L, Rahman R, Brundler MA, et al. Multifactorial analysis of predictors of outcome in pediatric intracranial ependymoma. *Neuro Oncol*. 2008;10:675–689.
31. Johnson RA, Wright KD, Poppleton H, et al. Cross-species genomics matches driver mutations and cell compartments to model ependymoma. *Nature*. 2010; 466:632–636.
32. Gibson P, Tong Y, Robinson G, et al. Subtypes of medulloblastoma have distinct developmental origins. *Nature*. 2010; 468:1095–1099.
33. Ling V. Multidrug resistance: molecular mechanisms and clinical relevance. *Cancer Chemother Pharmacol*. 1997;40(Suppl):S3–S8.
34. Pfister S, Remke M, Castoldi M, et al. Novel genomic amplification targeting the microRNA cluster at 19q13.42 in a pediatric embryonal tumor with abundant neuropil and true rosettes. *Acta Neuropathol*. 2009;117:457–464.
35. Korshunov A, Remke M, Gessi M, et al. Focal genomic amplification at 19q13.42 comprises a powerful diagnostic marker for embryonal tumors with ependymoblastic rosettes. *Acta Neuropathol*. 2010;120:253–260.
36. Gessi M, Giangaspero F, Lauriola L, et al. Embryonal tumors with abundant neuropil and true rosettes: a distinctive CNS primitive neuroectodermal tumor. *Am J Surg Pathol*. 2009;33:211–217.
37. Caren H, Erichsen J, Olsson L, et al. High-resolution array copy number analyses for detection of deletion, gain, amplification and copy-neutral LOH in primary neuroblastoma tumors: four cases of homozygous deletions of the CDKN2A gene. *BMC Genomics*. 2008;9:353.
38. Mendrzyk F, Radlwimmer B, Joos S, et al. Genomic and protein expression profiling identifies CDK6 as novel independent prognostic marker in medulloblastoma. *J Clin Oncol*. 2005;23:8853–8862.
39. Holtkamp N, Ziegenhagen N, Malzer E, Hartmann C, Giese A, von Deimling A. Characterization of the amplicon on chromosomal segment 4q12 in glioblastoma multiforme. *Neuro Oncol*. 2007;9:291–297.
40. Rossi MR, Conroy J, McQuaid D, Nowak NJ, Rutka JT, Cowell JK. Array CGH analysis of pediatric medulloblastomas. *Genes Chromosomes Cancer*. 2006;45:290–303.
41. Schiffman JD, Wang Y, McPherson LA, et al. Molecular inversion probes reveal patterns of 9p21 deletion and copy number aberrations in childhood leukemia. *Cancer Genet Cytogenet*. 2009;193:9–18.
42. Liggett WH, Jr, Sidransky D. Role of the p16 tumor suppressor gene in cancer. *J Clin Oncol*. 1998;16:1197–1206.
43. Barrow J, Adamowicz-Brice M, Cartmill M, et al. Homozygous loss of ADAM3A revealed by genome-wide analysis of pediatric high-grade glioma and diffuse intrinsic pontine gliomas. *Neuro Oncol*. 2011;13:212–222.

44. Taylor MD, Poppleton H, Fuller C, et al. Radial glia cells are candidate stem cells of ependymoma. *Cancer Cell*. 2005;8:323–335.
45. Dyer S, Prebble E, Davison V, et al. Genomic imbalances in pediatric intracranial ependymomas define clinically relevant groups. *Am J Pathol*. 2002;161:2133–2141.
46. Scotting PJ, Walker DA, Perilongo G. Childhood solid tumours: a developmental disorder. *Nat Rev Cancer*. 2005;5:481–488.
47. Biegel JA, Rorke LB, Packer RJ, et al. Isochromosome 17q in primitive neuroectodermal tumors of the central nervous system. *Genes Chromosomes Cancer*. 1989;1:139–147.
48. Lo KC, Rossi MR, Eberhart CG, Cowell JK. Genome wide copy number abnormalities in pediatric medulloblastomas as assessed by array comparative genome hybridization. *Brain Pathol*. 2007;17:282–296.
49. Michiels EM, Weiss MM, Hoovers JM, et al. Genetic alterations in childhood medulloblastoma analyzed by comparative genomic hybridization. *J Pediatr Hematol Oncol*. 2002;24:205–210.
50. Clifford SC, Lusher ME, Lindsey JC, et al. Wnt/Wingless pathway activation and chromosome 6 loss characterize a distinct molecular subgroup of medulloblastomas associated with a favorable prognosis. *Cell Cycle*. 2006;5:2666–2670.
51. Thompson MC, Fuller C, Hogg TL, et al. Genomics identifies medulloblastoma subgroups that are enriched for specific genetic alterations. *J Clin Oncol*. 2006;24:1924–1931.
52. Aldosari N, Bigner SH, Burger PC, et al. MYCC and MYCN oncogene amplification in medulloblastoma: a fluorescence in situ hybridization study on paraffin sections from the Children's Oncology Group. *Arch Pathol Lab Med*. 2002;126:540–544.
53. Eberhart CG, Kratz JE, Schuster A, et al. Comparative genomic hybridization detects an increased number of chromosomal alterations in large cell/anaplastic medulloblastomas. *Brain Pathol*. 2002;12:36–44.
54. Neben K, Korshunov A, Benner A, et al. Microarray-based screening for molecular markers in medulloblastoma revealed STK15 as independent predictor for survival. *Cancer Res*. 2004;64:3103–3111.